Bacterially Grown Cellulose/Graphene Oxide Composites Infused with γ-Poly (Glutamic Acid) as Biodegradable Structural Materials with Enhanced Toughness

Yu, Kui; Aubin-Tam, Marie Eve

DOI
10.1021/acsanm.0c02565

Publication date
2020

Document Version
Final published version

Published in
ACS Applied Nano Materials

ACS APPLIED NANO MATERIALS

www.acsanm.org

Article

Bacterially Grown Cellulose/Graphene Oxide Composites Infused with γ-Poly (Glutamic Acid) as Biodegradable Structural Materials with Enhanced Toughness

Kui Yu and Marie-Eve Aubin-Tam*

Cite This: *ACS Appl. Nano Mater.* 2020, 3, 12055−12063

Read Online

ACCESS | Metrics & More | Article Recommendations | Supporting Information

ABSTRACT: Bioinspired bacterial cellulose (BC) composites are next-generation renewable materials that exhibit promising industrial applications. However, large-scale production of inorganic/organic BC composites by *in situ* fermentation remains difficult. The methods based on BC mechanical disintegration impair the mechanical property of dried BC films, while the static *in situ* fermentation methods fail to incorporate inorganic particles within the BC network because of the limited diffusion ability. Furthermore, the addition of other components in the fermentation medium significantly interferes with the production of BC. Here, a tough BC composite with a layered structure reminiscent of the tough materials found in nature (*e.g.*, nacre, dentin, and bone) is prepared using a semistatic *in situ* fermentation method. The bacterially produced biopolymer γ-poly(glutamic acid) (PGA), together with graphene oxide (GO), is introduced into the BC fermentation medium. The resulting dried BC−GO−PGA composite film shows high toughness (36 MJ m^{-3}), which makes it one of the toughest BC composite film reported. In traditional *in situ* fermentation methods, the addition of a second component significantly reduces the wet thickness of the final composites. However, in this report, we show that addition of both PGA and GO to the fermentation medium shows a synergistic effect in increasing the wet thickness of the final BC composites. By gently agitating the solution, GO particles get entrapped into the BC network, as the formed pellicles can move below the liquid level and the GO particles suspended in the liquid can be entrapped into the BC network. Compared to other methods, this method achieves high toughness while using a mild and easily scalable fabrication procedure. These bacterially produced composites could be employed in the next generation of biodegradable structural high-performance materials, construction materials, and tissue engineering scaffolds (tendon, ligament, and skin) that require high toughness.

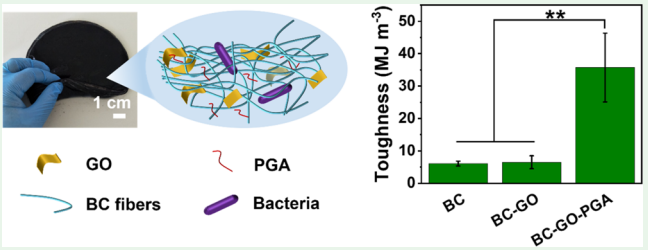

KEYWORDS: *bacterial cellulose, in situ fermentation, bioinspired materials, nacre, self-assembly, layered materials*

INTRODUCTION

With the increasing concern of environmental pollution, plastic waste, and energy shortage worldwide, the green fabrication of renewable bio-based materials is urgently needed.[1] Biodegradable biopolymers including polyesters [poly(hydroxyalkanoate) (PHA),[2] polylactide (PLA),[3] and polyethylene furanoate (PEF)[3]], polysaccharides [cellulose,[4] chitin,[5] and alginate[6]], and polyamides [γ-poly(glutamic acid) (PGA),[6] silk,[7] and collagen[8]] are drawing increasing attention. Among them, cellulose is the most abundant biopolymer found in nature.[9] Due to its hierarchical fibril structure and excellent mechanical strength, cellulose has become a desirable building block for the construction of high-performance structural materials.[4,10] However, plant-based cellulose is generally associated with hemicellulose, lignin, and pectin,[11] and the extraction of pure cellulose from the nature requires a chemically hazardous delignification process.[12] An environmentally friendly alternative is bacterial cellulose (BC), which is secreted by microorganisms (*e.g.*, *Acetobacter*[13]) in the form of a hydrogel-like pellicle.[14] In contrast to plant cellulose, BC is chemically pure (with almost 100% cellulose content[15]) and can be produced in a large scale at the air−liquid interface with a static fermentation method under mild conditions.[16] The BC pellicle consists of a layered nanofibrous microstructure,[11] a promising matrix substrate for making biomimetic materials.[17]

Although BC shows excellent mechanical performance, pure dried BC films lack certain properties such as high toughness values (over 5 MJ m^{-3})[18] and biocompatibility,[19] which limit their applications in various fields.[20] To endow dried BC films

Received: September 22, 2020
Accepted: November 23, 2020
Published: December 4, 2020

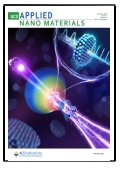

https://dx.doi.org/10.1021/acsanm.0c02565
ACS Appl. Nano Mater. 2020, 3, 12055−12063

with certain functions and broaden the possible applications, functional additives, including biopolymers[21] and inorganic particles, need to be incorporated into the fibrous network of BC.[22] The preparation of BC composites can be done with an *ex situ* method that involves mechanical crushing of the BC wet pellicle into a BC fiber dispersion and blending it with other components.[23−25] This method destroys the natural fibrous-layered structure of the BC pellicle and may impair the mechanical performance of the final BC composites. The mechanical disintegration may also reduce the tensile strength of dried reorganized BC films compared to dried pristine BC films.[26] To avoid this disadvantage, it is preferred to maintain the natural structure of BC. For incorporation of a second component into the BC structure, *in situ* impregnation[27] or vacuum filtration[28] methods are generally used. However, when it comes to viscous polymers, the vacuum filtration is time intensive, while the natural impregnation procedure without external force may result in an inhomogeneous polymer distribution in the BC network. Therefore, the incorporation of viscous polymers and inorganic particles without using toxic chemicals or external force into the BC fibrous network while maintaining its native structure is difficult but attractive for the fabrication of BC-based high-performance composites.

Static *in situ* fermentation provides a perfect solution to this problem. During the static fermentation process, water-soluble polymers or inorganic dispersions are added directly to the initial fermentation medium before the BC solid pellicle is formed.[20] The dissolved polymers or suspended particles are mixed together with the medium and thus become trapped into the newly formed BC fibril network, resulting in the formation of BC composites.[20] To incorporate inorganic particles into BC *via in situ* fermentation, sedimentation of inorganic particles should be avoided during the fermentation. Therefore, particles with abundant surface charges or polar groups, like graphene oxide (GO), are favorable. Also, the use of such additives may interfere with BC growth,[29,30] resulting in low yields and hence increased production costs for industrial applications.[29] The fabrication of inorganic particle-BC composites with a static *in situ* fermentation method has thus been restricted to thin films with an overall wet thickness smaller than 2 mm[31] because the particles can only remain suspended in the BC fermentation medium for a short time. After being precipitated, the particles cannot be entrapped in BC fibers at the surface.[20] Therefore, such static *in situ* fermentation methods fail to produce BC nanocomposites due to the limited diffusion of the nanoscale units from the liquid medium to the upper surface layer of growing BC.[26]

Here, a BC composite material with enhanced yield is produced under mild conditions by a semistatic *in situ* fermentation method (Figures 1, 2), where newly formed BC composite layers are shaken below the air−liquid interface once a day by simply moving the fermentation flask. A bacterially produced biopolymer, PGA, as well as GO is added to the initial fermentation medium. Due to the combined effect of PGA and GO, the yield (wet thickness) of the resulting material increases significantly. The yield is even slightly higher than when pure BC is produced, which is hardly achievable by other static *in situ* fermentation methods, where the wet thickness of the final composites is generally reduced after the addition of a second component in the initial fermentation medium. The resulting material shows a considerably high

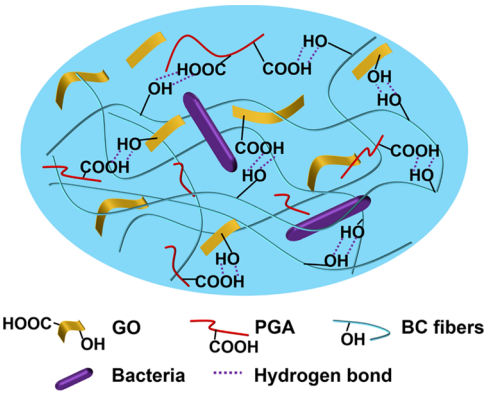

Figure 1. Schematic of the hydrogen bonding interactions among PGA, GO, and BC fibers.

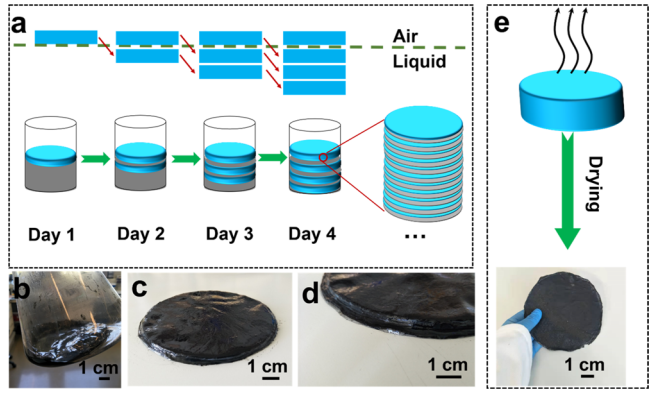

Figure 2. Fabrication procedure of the BC−GO−PGA composites. (a) Scheme of the fabrication method during the semistatic *in situ* fermentation, where the earlier formed layers are moved below the surface while the newly formed layers are formed at the air liquid interface; (b−d) optical images of the BC−GO−PGA composites after semistatic *in situ* fermentation; (e) BC−GO−PGA film after drying.

toughness (36 MJ m^{-3}), making it one of the toughest BC membrane reported so far. Compared to other methods, this membrane is fabricated under mild conditions and shows promising features for use as the next generation of biodegradable structural high-performance materials and construction materials and in tissue engineering applications (tendon, ligament, and skin) due to its enhanced yield and scalability.

RESULTS AND DISCUSSION

Fabrication of BC−GO−PGA Composites. Compared to *ex situ* methods,[23−25] *in situ* biofabrication methods[20] based on the addition of components into the initial fermentation medium are a straight-forward approach to incorporate other elements into the BC network. Water-soluble polymers[22,30] are widely used in static *in situ* BC fermentation since they mix readily with the bacterial medium and become trapped in the BC network. However, it is difficult to insert inorganic particles into the BC network as these particles tend to be unstable at the ionic strength required in the bacterial fermentation medium.[20] The agitated *in situ* fermentation method[32] keeps the inorganic particles suspended in the liquid medium and inserts these particles into the BC network during fermentation. However, this method can only produce small

https://dx.doi.org/10.1021/acsanm.0c02565
ACS Appl. Nano Mater. 2020, 3, 12055−12063

(usually less than 1 cm) BC pieces[33] that are dispersed in the solution instead of a bulk BC material.

To overcome these problems, we developed a semistatic *in situ* fermentation method (Figure 2a). In an Erlenmeyer flask, PGA and GO were mixed with Hestrin-Schramm (HS) medium. The fermentation was carried out at 30 °C under static conditions with the cellulose-producing strain *Gluconacetobacter hansenii* (*G. hansenii*). A thin layer of BC composites was formed at the air−liquid interface after 1 day of culturing. This thin layer can be submerged below the liquid level (Figure 2a) by simply shaking the Erlenmeyer flask once. The BC pellicle composites (Figure 2b−d) were obtained by daily repeating this static incubating and shaking procedure.

Compared to pure BC, the addition of PGA reduced the wet thickness of the resulting BC−PGA composite throughout the fermentation procedure (Figure 3a) from 5.4 ± 0.2 mm (day 5), 9.2 ± 0.5 mm (day 10), and 9.8 ± 0.6 mm (day 15) for BC alone to 1.7 ± 0.1 mm (day 5), 2.6 ± 0.1 mm (day 10), and 2.5 ± 0.2 mm (day 15) for the BC with PGA. Notably, there was no significant difference in wet thickness values between 10 and 15 days of fermentation (Figure 3a), both with and without PGA. Therefore, a period of 10 days was selected as the fermentation time for all other composites produced in this study.

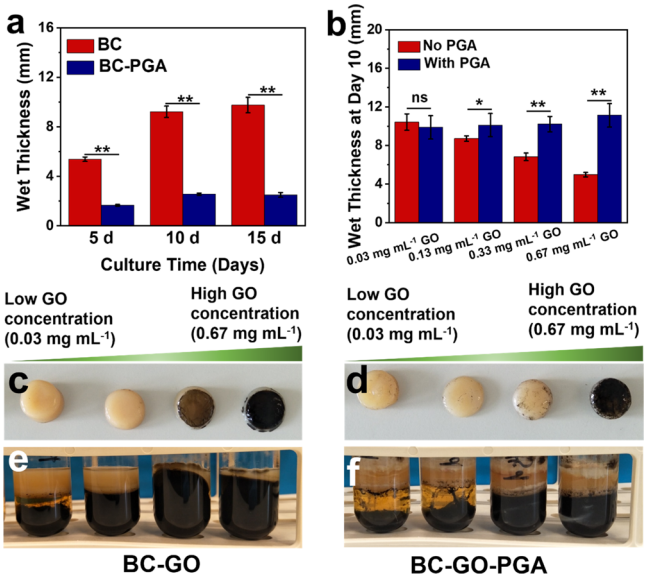

Figure 3. Yield of the BC−GO composites during *in situ* fermentation. (a) Wet thickness over the course of fermentation (with and without the addition of PGA) at different timepoints. (b) Comparison of the wet thickness with different GO concentrations in the initial fermentation medium (after 10 days of culturing). (c,d) Optical images of the BC−GO composites (bottom side, which is in contact with the liquid) without (c) and with (d) PGA at different GO concentrations (from left to right: 0.03, 0.13, 0.33, and 0.67 mg mL^{-1}) in the initial fermentation medium after 10 days of *in situ* fermentation. (e,f) Optical images of the fermentation broth without (e) and with (f) PGA after 10 days of static culturing. *$p < 0.05$, **$p < 0.01$, significant; ns: not significant.

To assess whether the GO content and the addition of PGA influence the yield of the composite materials produced, wet thicknesses were measured after 10 days of fermentation (Figure 3b). The wet thickness values dropped from 10 ± 1 mm to 5.0 ± 0.2 mm when the GO content in the fermentation medium was increased from 0.03 to 0.67 mg mL^{-1} without any PGA in the medium (Figures 3b,e, S1). Although higher yield (wet thickness) could be obtained at lower GO concentrations (0.03 mg mL^{-1}), sedimentation (Figure 3e,f) occurred at lower GO content (0.03 mg mL^{-1}) in the fermentation medium. At 0.03 mg mL^{-1} GO content, the bottom surface of the BC composite material, which is the surface in contact with the solution, showed a yellow color (Figure 3c, similar to that of pure BC), suggesting that the GO particles cannot be incorporated into the BC network. However, at higher GO concentration (0.67 mg mL^{-1}), the BC composites showed a black color on their bottom surface (Figure 3c), which indicates that GO particles were successfully incorporated into the BC network. Therefore, the entrapment of GO into the BC network only happens at high enough GO concentration, where the yield of the final composites is significantly reduced. These conflicting properties restrain the *in situ* biofabrication of BC−GO composites.

Interestingly, the addition of PGA to the fermentation medium resulted in the formation of BC−GO−PGA composites (Figures 3b,f, S1). The wet thickness of BC−GO−PGA composites showed similar values at low and high GO concentrations, that is, a thickness of 9.9 ± 1.2 mm at 0.03 mg mL^{-1} GO and 11 ± 1 mm at 0.67 mg mL^{-1} GO. Both BC−PGA (2.6 ± 0.1 mm) and BC−GO similarly showed reduced wet thicknesses compared to that of pure BC (9.2 ± 0.5 mm), while the synergistic addition of PGA together with GO resulted in an increase in wet thicknesses for BC−GO−PGA, reaching values varying from 9.9 ± 1.2 to 11 ± 1 mm (Figure 3b).

The synergistic effect of PGA and GO on the yield of the final composite can be explained by a reduction of BC crystallinity. The crystallization process was shown to be a rate-limiting step during BC production.[34] Negatively charged water-soluble polymers have been used as additives to enhance the yield by reducing BC crystallinity.[35] These polymers can absorb *via* hydrogen bonds onto BC microfibrils, and their negatively charged groups thus prevent the aggregation of BC microfibrils due to electrostatic repulsion.[36] In our situation, the addition of negatively charged PGA failed to increase the yield, most likely because it increased significantly the viscosity of the fermentation medium. The polymer viscosity influences the diffusion of water-soluble polymers into the BC microfibril network. When GO was added to the fermentation medium together with PGA, the medium viscosity was reduced compared to PGA alone, thus promoting the diffusion of PGA onto the surface of each BC microfibril, resulting in the reduction of crystallinity and the enhanced yield of the final composites.

At high GO concentration (0.67 mg mL^{-1}), BC−GO−PGA showed enhanced yield (Figure 3b), and GO particles could be entrapped into the BC network (Figure 3d); however, only a small fraction of the full thickness of BC−GO−PGA composites presented a mixed structure, manifested by a black color (Figure 3c−f). This is because the top layer of the composite (Figure 3e,f) was not in contact with GO in the fermentation medium.

To solve this problem, we used a semistatic fermentation method (Figure 2). After one day of static culturing, a thin layer of BC−GO−PGA composite was formed. We then gently shook the flask containing this thin layer of BC−GO−PGA film at the air-liquid interface to position the film below the liquid level and left the fermentation flask static for another day. This allowed the grown BC to contact the GO-containing

https://dx.doi.org/10.1021/acsanm.0c02565
ACS Appl. Nano Mater. 2020, 3, 12055−12063

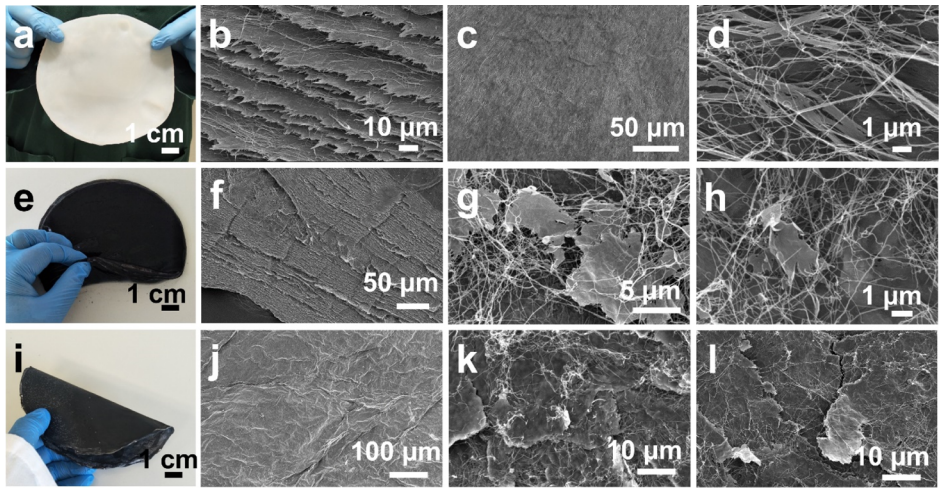

Figure 4. Characterization of layered composites. (a) BC−PGA wet hydrogel by *in situ* fermentation before drying. SEM images of (b) the cross section, (c) surface morphology, and (d) fiber morphology of the BC−PGA composite material after drying. *In situ*-fermented BC−PGA−GO composite material (e) before and (i) after drying. SEM images of (f−h) the cross-section morphology and (j−l) the surface morphology of the *in situ* fermented BC−GO−PGA composites after drying in air.

fermentation medium and form new BC−GO−PGA layers. After 10 days of daily treatment (once a day), BC−GO−PGA composites could be formed, with a completely colored hydrogel-like morphology (Figures 2b−d, 4e).

Morphology of the BC−GO−PGA Composites. After an *in situ* fermentation procedure, the fermented BC composites would normally be purified following the traditional BC purification method, where BC pellicles are boiled with 1 w/v % of sodium hydroxide (NaOH) solution and washed with distilled water.[37] This method, however, might result in the loss of PGA during the washing step due to its water-soluble nature.[38] To keep PGA within the fermented BC network, we used a calcium chloride ($CaCl_2{\cdot}2H_2O$) solution, instead of NaOH, when boiling the fermented composites. During this process, calcium ions (Ca^{2+}) can bind with the carboxyl groups (−COOH) in the PGA backbone to form a complex that resists solubilization in water. Fourier-transform infrared spectroscopy (FTIR) results (Figure S2) confirm the presence of PGA in the final composites. Furthermore, "freezing−thawing" (FT) procedures have been proven to be an effective way of improving the crystallinity and tensile properties of BC composites.[39] Therefore, after the boiling procedure with Ca^{2+},[40] we treated our specimens with a FT process, where the BC composites were placed inside a −20 °C freezer during 24 hours and then thawed at room temperature for 6 h. After repeating this FT process 5 times, the BC composites were washed with water until the pH of the water reaches 7. Hereafter, we refer to this whole post-treatment procedure as "CaFT". After this CaFT procedure, the BC wet pellicles were air-dried in the fume hood to form the final composite material (Figures 2e, 4i).

The addition of PGA did not influence the optical appearance of BC, with both BC−PGA−CaFT (Figure 4a) and pure BC (Figure S3) showing a white hydrogel-like appearance. Scanning electron microscope (SEM) images of BC−PGA−CaFT (Figure 4b−d) showed layered nanofibrous structures comparable to that of pure BC (Figure S4). However, after the addition of GO in the fermentation medium, the BC−GO−PGA−CaFT samples obtained *via* the semistatic method showed a black color due to the insertion of GO in the BC matrix (Figure 4e,i). SEM images of BC−GO−PGA−CaFT (Figure 4f−h,j−l) showed that GO particles are inserted into the layered nanofibrous network of BC, with GO being entangled and associated with BC nanofibers (Figure 4g,h,k,l). It should be noted that dried BC−GO−PGA−CaFT films showed a wrinkled surface morphology (Figure 4j), while the surface morphology of dried BC−PGA−CaFT films was rather smooth (Figure 4c). The formation of this wrinkled structure in the GO-containing sample is likely due to the large surface area of GO flakes, which tend to become curly and aggregate and absorb on the surface of BC fibers.[41,42]

Thermogravimetric analysis (TGA) curves (Figure S5) showed that the residual mass values of BC−GO−CaFT and BC−GO−PGA−CaFT lie between the ones of pure GO and BC−PGA−CaFT, confirming the presence of GO in the final composites. The GO content in the final composites can be calculated based on the residual mass ratio of TGA curves,[26] and the dried BC−GO−PGA films showed a 48.3% wt GO content. X-ray diffraction (XRD) analysis (Figure S6) revealed that the peaks present in the BC−GO−PGA−CaFT sample become less sharp compared to those of BC−PGA−CaFT, thus further confirming the presence of GO in the final composites.

Tensile Properties of the BC−GO−PGA Composites. To assess whether the post-treatment methods have any influence on the mechanical properties of BC−PGA composites, tensile tests were carried out. After 10 days of static fermentation in the presence of PGA, the BC wet pellicles were treated using 4 different methods: (1) by simply boiling in water (BC−PGA−water), (2) by boiling in a $CaCl_2{\cdot}2H_2O$ solution (BC−PGA−Ca), (3) by boiling in water followed by the FT procedure (BC−PGA−FT), or (4) by a combination of boiling in a $CaCl_2{\cdot}2H_2O$ solution followed by the FT procedure (BC−PGA−CaFT). The tensile tests (Figure 5a) show that the CaFT post-treatment procedure increased both the ultimate tensile strength and the elongation at break of the BC−PGA composites significantly. Compared to BC−PGA boiled in water (BC−PGA−water), BC−PGA−CaFT showed a ∼40% increase in ultimate tensile strength (from 180 ± 20 to 250 ± 20 MPa) and a ∼70% increase in elongation at break (from 5.1 ± 0.8 to 8.7 ± 0.5%) (Table S1). Due to the beneficial effect of CaFT on tensile properties of

https://dx.doi.org/10.1021/acsanm.0c02565
ACS Appl. Nano Mater. 2020, 3, 12055−12063

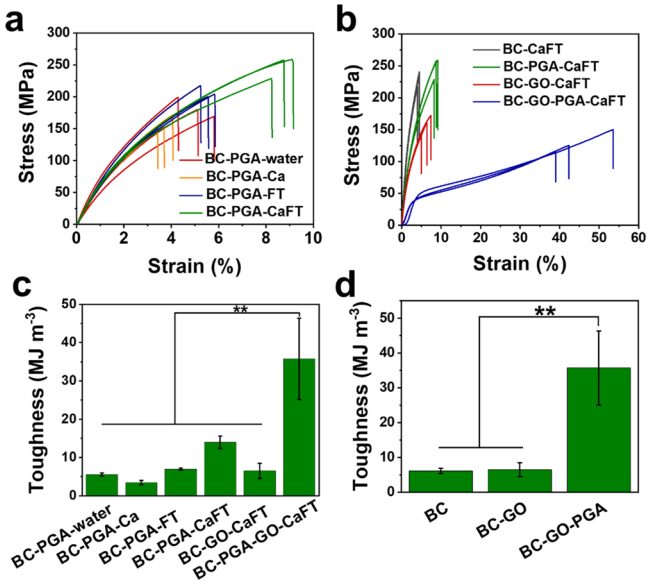

Figure 5. Tensile properties of the composite materials. (a) Stress–strain curves of BC–PGA composites with different post-treatment methods after *in situ* fermentation. (b) Stress–strains curves of the fermented composites after CaFT treatment. (c) Comparison of toughness values of the BC–GO–PGA composite with other specimens. (d) Comparison of toughness values of BC, BC–GO, and BC–GO–PGA. These three specimen types are treated with CaFT. $^{**}p < 0.01$, significant.

BC–PGA composites, all the GO-containing specimens were post-treated with the CaFT method.

From the previous analysis, we could demonstrate that GO inserted into the BC network when the GO content in the initial fermentation broth was 0.67 mg mL^{-1}; therefore, we used 0.67 mg mL^{-1} of GO here. After 10 days of semistatic *in situ* fermentation, BC–GO composites with and without PGA were post-treated with the CaFT procedure. Tensile tests (Figure 5b) revealed that BC–GO–PGA–CaFT showed a significant increase in the elongation at break value (45 ± 8%) compared to BC–CaFT (4.3 ± 0.3%), BC–PGA–CaFT (8.7 ± 0.5%), and BC–GO–CaFT (8.7 ± 0.5%). A lower elastic modulus value was obtained for dried BC–GO–PGA–CaFT films (1.8 ± 0.4 GPa, Table S1) compared to BC–PGA–CaFT (7.2 ± 2.2 GPa) and BC–CaFT (10 ± 2 GPa). Furthermore, the overall toughness value of BC–GO–PGA–CaFT reached up to 36 ± 11 MJ m^{-3}, which is significantly higher than all other specimens (Figure 5c,d, Table S1).

The considerably higher toughness for dried BC–GO–PGA–CaFT film samples is explained by the higher elongation at break. To understand the underlying mechanism behind this increase in elongation at break, the cross-section morphology of dried BC–GO–PGA–CaFT films after tensile testing was examined (Figure 6). Instead of a catastrophic failure, dried BC–GO–PGA–CaFT films showed a progressive failure morphology, with layer sliding[43] (Figure 6a–c), peel off[44] (Figure 6d–f), and pull out[43] (Figure 6g–i) morphologies observed. Additionally, dried BC–GO–PGA–CaFT films showed a wrinkled surface morphology (Figure 4j), and during the tensile testing, the wrinkles might extend and absorb energy, thus increasing the elongation at break. Therefore, the wrinkled structure might also be one of the reasons for the high toughness values. Moreover, the addition of PGA itself can also contribute to the increase in toughness, as shown previously for other types of composites,[45,46] since BC–PGA–CaFT showed higher toughness (Table S1, 14 ± 2 MJ m^{-3}) than BC–CaFT (6.1 ± 0.8 MJ m^{-3}). In summary, the combined effects of several mechanisms including a progressive failure accompanied by layer sliding, peel off and pull out, a wrinkled morphology, as well as the addition of PGA, could all contribute to the fact that the dried BC–GO–PGA–CaFT film was significantly tougher compared to the other specimens.

Comparison with Other BC-Based Materials. Because of its layered nanofibrous structure and its mild and scalable production capability, BC draws increasing attention for the fabrication of bioinspired high-performance structural materials.[17,47,48] To insert other components into the BC fibrous network, multiple methods, including mechanical disintegration,[23−25] *in situ* post impregnation,[37] *in situ* vacuum filtration,[28] and *in situ* fermentation,[48] are being developed. Among these methods, *in situ* fermentation is the most promising method,[20] as it is less energy consuming, carried out in mild conditions, and can easily achieve an homogeneous distribution of other components into the BC network.

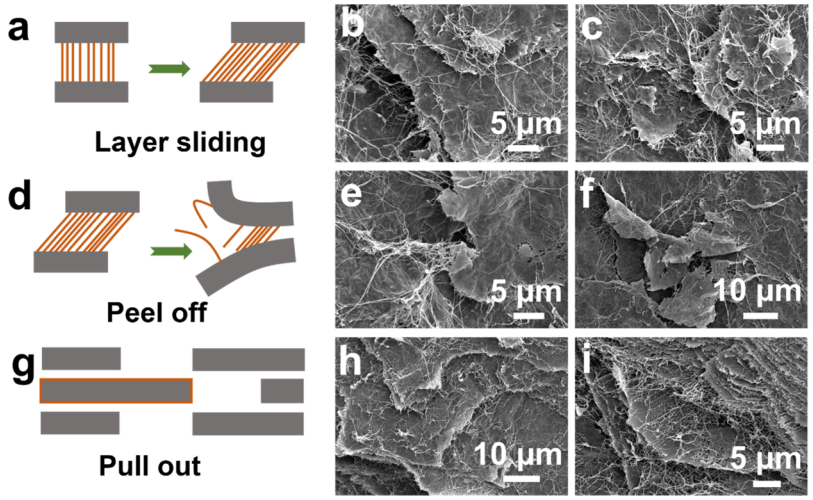

Figure 6. Proposed breaking mechanism of the BC–GO–PGA composites. (a–c) Layer sliding, (d–f) peel off and (g–i) pull out morphologies are observed from SEM of the failure cross-section.

https://dx.doi.org/10.1021/acsanm.0c02565
ACS Appl. Nano Mater. 2020, 3, 12055−12063

However, it is problematic to insert inorganic particles into the BC network with a static *in situ* fermentation method due to the limited diffusion of these particles to the air−liquid interface.[26] Compared to all these BC composite fabrication methods, the semistatic *in situ* fermentation method in this study provides an easily implemented approach to incorporate inorganic particles into a BC nanofibrous network. Due to the addition of PGA, the yield of the final composite material increases significantly and the BC−GO−PGA shows a relatively high yield compared to other BC-based composites produced *via in situ* fermentation (Table S2). The BC−GO−PGA−CaFT specimens show an excellent toughness value (36 MJ m^{-3}), which is among the highest reported for BC composites and BC-based high performance materials so far (Table 1).

Table 1. Comparison of Toughness Values Among the Cellulose-Based Film Materials

type of cellulose-based film	tensile toughness[a] [MJ m^{-3}]	refs
alkali treated cellulose	6.3	49
BC−GO	8.2	47
CNF (cellulose nanofiber)−GO	14.2	50
wet stretched and hot pressed BC	24.7	51
double-cross-linked cellulose	28.2	52
hot pressed and tap-peeled BC	36.4	53
anisotropic plant cellulose	41.1	54
BC−PGA−CaFT	14	this work
BC−GO−PGA−CaFT	36	this work

[a]The tensile testing is influenced by many factors including the sample geometry, porosity, moisture content, grammage, and testing conditions.[55]

CONCLUSIONS

A BC−GO−PGA composite material with a bioinspired layered morphology was prepared following a semistatic *in situ* fermentation method. This BC−GO−PGA composite material is one of the toughest BC composite membranes reported. GO particles were inserted successfully into the BC nanofibrous structure by a daily shaking procedure. Notably, after the addition of the bacterial polymer PGA, the yield (wet thickness) of the final BC composites increased significantly, which is hardly achievable by other static *in situ* fermentation methods, where the wet thickness of the final composites is generally reduced after the addition of components in the initial fermentation medium. Compared to other methods, this approach is mild and easily scalable. BC and PGA are both bacterially produced, making this an environmentally friendly biofabrication method for bioinspired high-performance structural materials. Due to these advantages, this material shows promising applications as protective garments or as biodegradable structural high-performance materials, construction materials, and tissue engineering scaffolds (tendon, ligament, and skin) that require high toughness.

EXPERIMENTAL SECTION

Materials, Strain, and Medium. D(+)-glucose monohydrate and di-sodium hydrogen phosphate (≥99.0%) were obtained from Carl Roth GmbH. Other chemicals were purchased from Sigma-Aldrich.

The cellulose producing strain *G. hansenii* (ATCC 53582) was inoculated in HS medium (5.0 g L^{-1} tryptone, 5.0 g L^{-1} yeast extract, 2.7 g L^{-1} disodium hydrogen phosphate, 1.5 g L^{-1} citric acid, and 20 g L^{-1} glucose) at 30 °C under static conditions for 3 days to obtain the BC pellicle at the air−liquid interface. The inoculum for bacterial fermentation was prepared by treating the BC pellicle with cellulase from *Trichoderma reesei* (aqueous solution, ≥ 700 units g^{-1}) on a shaking platform at 180 rpm at 30 °C overnight. The solution was then centrifuged (4 °C, 3220 ×*g* centrifuge speed, 5 min) to remove the cellulase and supernatant, and the bacterial pellet was resuspended in fresh HS medium to obtain an OD_{600} of 1. A 1 v/v % of this solution was then used as the inoculum.

Preparation of Bacterial PGA. Overnight cultures of *Bacillus licheniformis* (*B. licheniformis* NBRC12107, NBRC, Japan) grown in BL medium (10 g L^{-1} peptone, 2 g L^{-1} yeast extract, and 1 g L^{-1} $MgSO_4·H_2O$) (1.5 v/v %) were added to autoclaved PGA production medium (20 g L^{-1} L-glutamic acid, 13.6 g L^{-1} sodium citrate monobasic, 80 g L^{-1} glycerol, 7 g L^{-1} NH_4Cl, 0.5 g L^{-1} KH_2PO_4, 0.244 g L^{-1} $MgSO_4$, 0.04 g L^{-1} $FeCl_3·6H_2O$, 0.15 g L^{-1} $CaCl_2·2H_2O$, and 0.1 g L^{-1} $MnSO_4·H2O$; pH was adjusted to 7.5) and incubated at 30 °C for 48 h on a platform shaking at 180 rpm. After incubation, the formed viscous PGA solution was centrifuged at × 8200*g* for 15 min at 4 °C to remove the bacteria. The polymer solution was mixed with over twice the volume of ethanol. The precipitated PGA polymer was then dried in the oven at 50 °C for 2 days. The dried PGA solid polymer was UV-treated overnight and dissolved into sterilized distilled water at 1 w/v % concentration for use.

Preparation of the Fermentation Medium. The total volume of the fermentation medium was fixed at 12 mL. 8 mL of HS medium and 120 μL of bacteria were added to each glass tube. For the samples with PGA, 2 mL of 1 w/v % PGA solution was added. 0.05, 0.1, 0.5, or 1 mL of 8 mg mL^{-1} GO solutions were added to different tubes. Finally, sterilized distilled water was added to make sure that the total volume in each tube was exactly 12 mL. These fermentation broths with different GO concentrations (0.03, 0.13, 0.33, and 0.67 mg mL^{-1}) were then incubated at 30 °C for 24 h.

Semistatic *In Situ* Fermentation. The above GO-containing fermentation broths were incubated at 30 °C in static conditions. After a period of 24 h, a thin film formed at the air−liquid interface. The incubation flask was gently shaken so that the solid BC pellicle was submerged below the liquid level, and the flask was left in a static position for another 24 h of fermentation. This procedure was repeated daily until the end of the fermentation. The BC pellicle remained close to the air−liquid interface after being shaken gently, likely due to the presence of BC nanofibers in the liquid (Figure S7), which increased the density of the liquid. Unless specified, all BC pellicles in this study were prepared following this semistatic *in situ* fermentation method.

Post-treatment of the Composites. After fermentation, the solid pellet was transferred into a beaker and filled with 200 mL of 1 M $CaCl_2·2H_2O$ solution. The pellet was boiled on a heating plate for 10 min to kill the bacteria. After cooling down, the pellet was transferred into a −20 °C freezer for 24 h and then thawed at room temperature for 6 h. After repeating this FT process 5 times, the BC composites were washed with water until the pH of the water reached 7. After this "CaFT" procedure, the BC wet pellicles were dried in the fume hood for 7 days to form the resulting composites and stored in a glass desiccator with reduced pressure for further testing. To check the moisture content, the air-dried films were further oven-dried at 50 °C for 48 h. The air-dried films showed similar morphology and moisture content compared to the air-and-oven-dried films (Figure S8).

Characterization of the BC Composites. The wet thicknesses of the different composite pellicles of varying culturing times were measured with a Vernier caliper.

The materials' morphology was observed by SEM (JEOL JSM 6010 LA). The material was sputter-coated with gold-palladium at 20 mA for 60 s and was observed at 5−15 kV with SEI mode under vacuum.

FTIR (PerkinElmer, Spectrum 100) equipped with an attenuated total reflection (ATR) accessory was carried out with the average of 20 scans in the 550−4000 cm^{-1} range at a resolution of 4 cm^{-1}.

https://dx.doi.org/10.1021/acsanm.0c02565
ACS Appl. Nano Mater. 2020, 3, 12055−12063

TGA (Mettler Toledo) was performed at 30−1000 °C with a heating rate of 10 °C min^{-1} in a nitrogen atmosphere. The GO content in the final dried BC−GO−PGA film was calculated by TGA[26] according to eq 1

$$\text{wt \%}_{(GO)} = \frac{\varphi_0 - \varphi_{polymer}}{\varphi_{GO} - \varphi_{polymer}} \times 100\% \quad (1)$$

where φ_0 is the total residual ratio of TGA for the dried BC−GO−PGA film under a nitrogen atmosphere, $\varphi_{polymer}$ is the residual ratio of the dried BC−PGA film under the same measurement conditions, and φ_{GO} is the residual ratio of pure GO under the same testing conditions.

XRD (Bruker D8 ADVANCE, Bruker AXS) was carried out by an Ultima III X-ray diffractometer (Rigaku Co. Ltd., Japan). Ni-filtered Cu Kα radiation (λ = 0.1542 nm) was generated from 40 kV voltage and 40 mA current, with a LynyEye detector, Cobalt (with Iron filter) source, Bragg Brentano (reflection mode) geometry, a step size of 0.02°, and a scan speed of 2°/min between 2θ = 5−60°.

Tensile Testing. For tensile strength testing, the samples were prepared by drying the wet pellicle in a fume hood during 7 days. These dried films were cut into rectangular shapes with dimensions of 50 × 7 mm^2 and stored into a glass desiccator with reduced pressure before tensile testing. The tensile testing was performed using a Zwick/Roell Z010 universal testing machine with a 500 N load cell and 1 kN grips. The grip distance was 10 mm, and the tests were carried out with a loading rate of 2 mm min^{-1} under ambient lab conditions, with a temperature of 23 °C and 45% humidity. The specimen information can be found in the Supporting Information (Table S3). The grammage of the final dried BC film was calculated by the ratio of mass and its measured area.[56]

Porosity. The porosity was measured by an ethanol immersion method.[57] Briefly, a 10 mm × 30 mm dried film was immersed into a 10 mL measuring cylinder with ethanol. The volumes in the cylinder were measured before (V_1) and after (V_2) film immersion. After 15 min, the film was removed from the ethanol, and the remaining volume (V_3) was measured. The porosity of the film was calculated according to the eq 2

$$\text{Porosity (\%)} = \frac{V_1 - V_3}{V_2 - V_3} \times 100\% \quad (2)$$

Statistics. Statistical analyses were performed on https://astatsa.com/. The experimental groups were compared using one-way (single factor) ANOVA with post-hoc Tukey's HSD (honest significant difference) tests.

■ ASSOCIATED CONTENT

Supporting Information

The Supporting Information is available free of charge at https://pubs.acs.org/doi/10.1021/acsanm.0c02565.

Optical images of BC and composites; FTIR; TGA; XRD; SEM of BC; tensile properties; dry weight yield of BC composites; and parameters for the tensile tests (PDF)

■ AUTHOR INFORMATION

Corresponding Author

Marie-Eve Aubin-Tam − *Department of Bionanoscience, Kavli Institute of Nanoscience, Delft University of Technology, 2629 HZ Delft, The Netherlands;* orcid.org/0000-0001-9995-2623; Email: M.E.Aubin-Tam@tudelft.nl

Author

Kui Yu − *Department of Bionanoscience, Kavli Institute of Nanoscience, Delft University of Technology, 2629 HZ Delft, The Netherlands;* orcid.org/0000-0003-3673-8843

Complete contact information is available at: https://pubs.acs.org/10.1021/acsanm.0c02565

Notes

The authors declare no competing financial interest.

■ ACKNOWLEDGMENTS

The authors thank Mascha Slingerland and Tessa Essers for their help with the tensile testing, Marlies Nijemeisland for FTIR, Xiaohui Liu and Ben Norder for XRD, and Bart van der Linden for the TGA measurements. We thank Kuang Liang for the discussion about GO. We thank Srikkanth Balasubramanian and Ramon van der Valk for their comments on the manuscript. K.Y. is funded by the China Scholarship Council (CSC no. 201706630001).

■ REFERENCES

(1) Mohanty, A. K.; Vivekanandhan, S.; Pin, J.-M.; Misra, M. Composites from Renewable and Sustainable Resources: Challenges and Innovations. *Science* **2018**, *362*, 536.

(2) Meereboer, K. W.; Misra, M.; Mohanty, A. K. Review of Recent Advances in the Biodegradability of Polyhydroxyalkanoate (PHA) Bioplastics and Their Composites. *Green Chem.* **2020**, *22*, 5519−5558.

(3) Zhu, Y.; Romain, C.; Williams, C. K. Sustainable Polymers from Renewable Resources. *Nature* **2016**, *540*, 354−362.

(4) Ray, U.; Zhu, S.; Pang, Z.; Li, T. Mechanics Design in Cellulose-Enabled High-Performance Functional Materials. *Adv. Mater.* **2020**, 2002504.

(5) Bai, L.; Kämäräinen, T.; Xiang, W.; Majoinen, J.; Seitsonen, J.; Grande, R.; Huan, S.; Liu, L.; Fan, Y.; Rojas, O. J. Chirality from Cryo-Electron Tomograms of Nanocrystals Obtained by Lateral Disassembly and Surface Etching of Never-Dried Chitin. *ACS Nano* **2020**, *14*, 6921−6930.

(6) Moradali, M. F.; Rehm, B. H. A. Bacterial Biopolymers: From Pathogenesis to Advanced Materials. *Nat. Rev. Microbiol.* **2020**, *18*, 195−210.

(7) Yoshioka, T.; Tsubota, T.; Tashiro, K.; Jouraku, A.; Kameda, T. A Study of the Extraordinarily Strong and Tough Silk Produced by Bagworms. *Nat. Commun.* **2019**, *10*, 1469.

(8) Ling, S.; Chen, W.; Fan, Y.; Zheng, K.; Jin, K.; Yu, H.; Buehler, M. J.; Kaplan, D. L. Biopolymer Nanofibrils: Structure, Modeling, Preparation, and Applications. *Prog. Polym. Sci.* **2018**, *85*, 1−56.

(9) Tu, H.; Zhu, M.; Duan, B.; Zhang, L. Recent Progress in High-Strength and Robust Regenerated Cellulose Materials. *Adv. Mater.* **2020**, 2000682.

(10) Kontturi, E.; Laaksonen, P.; Linder, M. B.; Nonappa; Gröschel, A. H.; Rojas, O. J.; Ikkala, O. Advanced Materials through Assembly of Nanocelluloses. *Adv. Mater.* **2018**, *30*, 1703779.

(11) Gromovykh, T. I.; Pigaleva, M. A.; Gallyamov, M. O.; Ivanenko, I. P.; Ozerova, K. E.; Kharitonova, E. P.; Bahman, M.; Feldman, N. B.; Lutsenko, S. V.; Kiselyova, O. I. Structural Organization of Bacterial Cellulose: The Origin of Anisotropy and Layered Structures. *Carbohydr. Polym.* **2020**, *237*, 116140.

(12) Khakalo, A.; Tanaka, A.; Korpela, A.; Orelma, H. Delignification and Ionic Liquid Treatment of Wood toward Multifunctional High-Performance Structural Materials. *ACS Appl. Mater. Interfaces* **2020**, *12*, 23532−23542.

(13) Florea, M.; Reeve, B.; Abbott, J.; Freemont, P. S.; Ellis, T. Genome Sequence and Plasmid Transformation of the Model High-Yield Bacterial Cellulose Producer Gluconacetobacter Hansenii ATCC 53582. *Sci. Rep.* **2016**, *6*, 23635.

(14) Gao, M.; Li, J.; Bao, Z.; Hu, M.; Nian, R.; Feng, D.; An, D.; Li, X.; Xian, M.; Zhang, H. A Natural In Situ Fabrication Method of Functional Bacterial Cellulose Using a Microorganism. *Nat. Commun.* **2019**, *10*, 437.

(15) Ma, L.; Bi, Z.; Xue, Y.; Zhang, W.; Huang, Q.; Zhang, L.; Huang, Y. Bacterial Cellulose: An Encouraging Eco-Friendly Nano-Candidate for Energy Storage and Energy Conversion. *J. Mater. Chem. A* **2020**, *8*, 5812−5842.
(16) Wang, J.; Tavakoli, J.; Tang, Y. Bacterial Cellulose Production, Properties and Applications with Different Culture Methods - A Review. *Carbohydr. Polym.* **2019**, *219*, 63−76.
(17) Guan, Q.-F.; Ling, Z.-C.; Han, Z.-M.; Yang, H.-B.; Yu, S.-H. Ultra-Strong, Ultra-Tough, Transparent, and Sustainable Nanocomposite Films for Plastic Substitute. *Matter* **2020**, *3*, 965−1376.
(18) Yu, K.; Balasubramanian, S.; Pahlavani, H.; Mirzaali, M. J.; Zadpoor, A. A.; Aubin-Tam, M.-E. Spiral Honeycomb Microstructured Bacterial Cellulose for Increased Strength and Toughness. *ACS Appl. Mater. Interfaces* **2020**, *12*, 50748−50755.
(19) de Oliveira Barud, H. G.; da Silva, R. R.; da Silva Barud, H.; Tercjak, A.; Gutierrez, J.; Lustri, W. R.; de Oliveira, O. B.; Ribeiro, S. J. L. A Multipurpose Natural and Renewable Polymer in Medical Applications: Bacterial Cellulose. *Carbohydr. Polym.* **2016**, *153*, 406−420.
(20) Shah, N.; Ul-Islam, M.; Khattak, W. A.; Park, J. K. Overview of Bacterial Cellulose Composites: A Multipurpose Advanced Material. *Carbohydr. Polym.* **2013**, *98*, 1585−1598.
(21) Eichhorn, S. J.; Dufresne, A.; Aranguren, M.; Marcovich, N. E.; Capadona, J. R.; Rowan, S. J.; Weder, C.; Thielemans, W.; Roman, M.; Renneckar, S.; Gindl, W.; Veigel, S.; Keckes, J.; Yano, H.; Abe, K.; Nogi, M.; Nakagaito, A. N.; Mangalam, A.; Simonsen, J.; Benight, A. S.; Bismarck, A.; Berglund, L. A.; Peijs, T. Review: Current International Research into Cellulose Nanofibres and Nanocomposites. *J. Mater. Sci.* **2010**, *45*, 1−33.
(22) Torres, F. G.; Arroyo, J. J.; Troncoso, O. P. Bacterial Cellulose Nanocomposites: An All-Nano Type of Material. *Mater. Sci. Eng., C* **2019**, *98*, 1277−1293.
(23) Fang, Q.; Zhou, X.; Deng, W.; Zheng, Z.; Liu, Z. Freestanding Bacterial Cellulose-Graphene Oxide Composite Membranes with High Mechanical Strength for Selective Ion Permeation. *Sci. Rep.* **2016**, *6*, 33185.
(24) Zhu, Z.-S.; Qu, J.; Hao, S.-M.; Han, S.; Jia, K.-L.; Yu, Z.-Z. Alpha- Fe_2O_3 Nanodisk/Bacterial Cellulose Hybrid Membranes as High-Performance Sulfate-Radical-Based Visible Light Photocatalysts under Stirring/Flowing States. *ACS Appl. Mater. Interfaces* **2018**, *10*, 30670−30679.
(25) Cabañas-Romero, L. V.; Valls, C.; Valenzuela, S. V.; Roncero, M. B.; Pastor, F. I. J.; Diaz, P.; Martínez, J. Bacterial Cellulose−Chitosan Paper with Antimicrobial and Antioxidant Activities. *Biomacromolecules* **2020**, *21*, 1568−1577.
(26) Guan, Q.-F.; Han, Z.-M.; Luo, T.-T.; Yang, H.-B.; Liang, H.-W.; Chen, S.-M.; Wang, G.-S.; Yu, S.-H. A General Aerosol-Assisted Biosynthesis of Functional Bulk Nanocomposites. *Natl. Sci. Rev.* **2019**, *6*, 64−73.
(27) Yano, H.; Sugiyama, J.; Nakagaito, A. N.; Nogi, M.; Matsuura, T.; Hikita, M.; Handa, K. Optically Transparent Composites Reinforced with Networks of Bacterial Nanofibers. *Adv. Mater.* **2005**, *17*, 153−155.
(28) Ccorahua, R.; Troncoso, O. P.; Rodriguez, S.; Lopez, D.; Torres, F. G. Hydrazine Treatment Improves Conductivity of Bacterial Cellulose/Graphene Nanocomposites Obtained by a Novel Processing Method. *Carbohydr. Polym.* **2017**, *171*, 68−76.
(29) Ruka, D. R.; Simon, G. P.; Dean, K. M. In Situ Modifications to Bacterial Cellulose with the Water Insoluble Polymer Poly-3-Hydroxybutyrate. *Carbohydr. Polym.* **2013**, *92*, 1717−1723.
(30) Chen, Y.; Zhou, X.; Lin, Q.; Jiang, D. Bacterial Cellulose/Gelatin Composites: In Situ Preparation and Glutaraldehyde Treatment. *Cellulose* **2014**, *21*, 2679−2693.
(31) Luo, H.; Dong, J.; Yao, F.; Yang, Z.; Li, W.; Wang, J.; Xu, X.; Hu, J.; Wan, Y. Layer-by-Layer Assembled Bacterial Cellulose/Graphene Oxide Hydrogels with Extremely Enhanced Mechanical Properties. *Nano-Micro Lett.* **2018**, *10*, 42.
(32) Nandgaonkar, A. G.; Wang, Q.; Fu, K.; Krause, W. E.; Wei, Q.; Gorga, R.; Lucia, L. A. A One-Pot Biosynthesis of Reduced Graphene Oxide (RGO)/Bacterial Cellulose (BC) Nanocomposites. *Green Chem.* **2014**, *16*, 3195−3201.
(33) Campano, C.; Balea, A.; Blanco, A.; Negro, C. Enhancement of the Fermentation Process and Properties of Bacterial Cellulose: A Review. *Cellulose* **2015**, *23*, 57−91.
(34) Haigler, C. H.; White, A. R.; Brown, R. M.; Cooper, K. M. Alteration of In Vivo Cellulose Ribbon Assembly by Carboxymethylcellulose and Other Cellulose Derivatives. *J. Cell Biol.* **1982**, *94*, 64−69.
(35) Cheng, K.-C.; Catchmark, J. M.; Demirci, A. Effect of Different Additives on Bacterial Cellulose Production by Acetobacter Xylinum and Analysis of Material Property. *Cellulose* **2009**, *16*, 1033−1045.
(36) Hirai, A.; Tsuji, M.; Yamamoto, H.; Horii, F. In Situ Crystallization of Bacterial Cellulose III. Infuences of Different Polymeric Additives on the Formation of Microfibrils as Revealed by Transmission Electron Microscopy. *Cellulose* **1998**, *5*, 201−213.
(37) Cazón, P.; Vázquez, M.; Velazquez, G. Environmentally Friendly Films Combining Bacterial Cellulose, Chitosan, and Polyvinyl Alcohol: Effect of Water Activity on Barrier, Mechanical, and Optical Properties. *Biomacromolecules* **2020**, *21*, 753−760.
(38) Cao, M.; Feng, J.; Sirisansaneeyakul, S.; Song, C.; Chisti, Y. Genetic and Metabolic Engineering for Microbial Production of Poly-Gamma-Glutamic Acid. *Biotechnol. Adv.* **2018**, *36*, 1424−1433.
(39) Millon, L. E.; Wan, W. K. The Poly Vinyl Alcohol-Bacterial Cellulose System as a New Nanocomposite for Biomedical Applications. *J. Biomed. Mater. Res., Part B* **2006**, *79*, 245−253.
(40) Butylina, S.; Geng, S.; Oksman, K. Properties of As-Prepared and Freeze-Dried Hydrogels Made from Poly(Vinyl Alcohol) and Cellulose Nanocrystals Using Freeze-Thaw Technique. *Eur. Polym. J.* **2016**, *81*, 386−396.
(41) Hu, K. M.; Liu, Y. Q.; Zhou, L. W.; Xue, Z. Y.; Peng, B.; Yan, H.; Di, Z. F.; Jiang, X. S.; Meng, G.; Zhang, W. M. Delamination-Free Functional Graphene Surface by Multiscale, Conformal Wrinkling. *Adv. Funct. Mater.* **2020**, *30*, 2003273.
(42) Liu, W.; Liu, N.; Yue, Y.; Rao, J.; Cheng, F.; Su, J.; Liu, Z.; Gao, Y. Piezoresistive Pressure Sensor Based on Synergistical Innerconnect Polyvinyl Alcohol Nanowires/Wrinkled Graphene Film. *Small* **2018**, *14*, 1704149.
(43) Wegst, U. G. K.; Bai, H.; Saiz, E.; Tomsia, A. P.; Ritchie, R. O. Bioinspired Structural Materials. *Nat. Mater.* **2015**, *14*, 23−36.
(44) Alsaadi, M.; Erkliğ, A. Effect of Perlite Particle Contents on Delamination Toughness of S-Glass Fiber Reinforced Epoxy Matrix Composites. *Composites, Part B* **2018**, *141*, 182−190.
(45) Spiesz, E. M.; Schmieden, D. T.; Grande, A. M.; Liang, K.; Schwiedrzik, J.; Natalio, F.; Michler, J.; Garcia, S. J.; Aubin-Tam, M. E.; Meyer, A. S. Bacterially Produced, Nacre-Inspired Composite Materials. *Small* **2019**, *15*, 1805312.
(46) Liang, K.; Spiesz, E. M.; Schmieden, D. T.; Xu, A. W.; Meyer, A. S.; Aubin-Tam, M. E. Bioproduced Polymers Self-Assemble with Graphene Oxide into Nanocomposite Films with Enhanced Mechanical Performance. *ACS Nano* **2020**, *14*, 14731−14739.
(47) Dhar, P.; Pratto, B.; Gonçalves Cruz, A. J.; Bankar, S. Valorization of Sugarcane Straw to Produce Highly Conductive Bacterial Cellulose / Graphene Nanocomposite Films through In Situ Fermentation: Kinetic Analysis and Property Evaluation. *J. Cleaner Prod.* **2019**, *238*, 117859.
(48) Dhar, P.; Etula, J.; Bankar, S. B. In Situ Bioprocessing of Bacterial Cellulose with Graphene: Percolation Network Formation, Kinetic Analysis with Physicochemical and Structural Properties Assessment. *ACS Appl. Bio Mater.* **2019**, *2*, 4052−4066.
(49) Nan, F.; Nagarajan, S.; Chen, Y.; Liu, P.; Duan, Y.; Men, Y.; Zhang, J. Enhanced Toughness and Thermal Stability of Cellulose Nanocrystal Iridescent Films by Alkali Treatment. *ACS Sustainable Chem. Eng.* **2017**, *5*, 8951−8958.
(50) Zhang, T.; Zhang, X.; Chen, Y.; Duan, Y.; Zhang, J. Green Fabrication of Regenerated Cellulose/Graphene Films with Simultaneous Improvement of Strength and Toughness by Tailoring the Nanofiber Diameter. *ACS Sustainable Chem. Eng.* **2017**, *6*, 1271−1278.

https://dx.doi.org/10.1021/acsanm.0c02565
ACS Appl. Nano Mater. 2020, 3, 12055−12063

(51) Wang, S.; Li, T.; Chen, C.; Kong, W.; Zhu, S.; Dai, J.; Diaz, A. J.; Hitz, E.; Solares, S. D.; Li, T.; Hu, L. Transparent, Anisotropic Biofilm with Aligned Bacterial Cellulose Nanofibers. *Adv. Funct. Mater.* **2018**, *28*, 1707491.
(52) Wei, P.; Huang, J.; Lu, Y.; Zhong, Y.; Men, Y.; Zhang, L.; Cai, J. Unique Stress Whitening and High-Toughness Double-Cross-Linked Cellulose Films. *ACS Sustainable Chem. Eng.* **2018**, *7*, 1707−1717.
(53) Wu, Z.; Chen, S.; Wu, R.; Sheng, N.; Zhang, M.; Ji, P.; Wang, H. Top-Down Peeling Bacterial Cellulose to High Strength Ultrathin Films and Multifunctional Fibers. *Chem. Eng. J.* **2020**, *391*, 123527.
(54) Ye, D.; Lei, X.; Li, T.; Cheng, Q.; Chang, C.; Hu, L.; Zhang, L. Ultrahigh Tough, Super Clear, and Highly Anisotropic Nanofiber-Structured Regenerated Cellulose Films. *ACS Nano* **2019**, *13*, 4843−4853.
(55) Hervy, M.; Santmarti, A.; Lahtinen, P.; Tammelin, T.; Lee, K.-Y. Sample Geometry Dependency on the Measured Tensile Properties of Cellulose Nanopapers. *Mater. Des.* **2017**, *121*, 421−429.
(56) Mautner, A.; Nawawi, W. M. F. W.; Lee, K.-Y.; Bismarck, A. High Porosity Cellulose Nanopapers as Reinforcement in Multi-Layer Epoxy Laminates. *Composites, Part A* **2020**, *131*, 105779.
(57) Yu, K.; Zhou, X.; Zhu, T.; Wu, T.; Wang, J.; Fang, J.; El-Aassar, M. R.; El-Hamshary, H.; El-Newehy, M.; Mo, X. Fabrication of Poly(Ester-Urethane)Urea Elastomer/Gelatin Electrospun Nanofibrous Membranes for Potential Applications in Skin Tissue Engineering. *RSC Adv.* **2016**, *6*, 73636−73644.

https://dx.doi.org/10.1021/acsanm.0c02565
ACS Appl. Nano Mater. 2020, 3, 12055−12063